Mechanical Systems and Signal Processing 101 (2018) 197–210

Contents lists available at ScienceDirect

Mechanical Systems and Signal Processing

journal homepage: www.elsevier.com/locate/ymssp

On the use of temperature for online condition monitoring of geared systems – A review

T. Touret [a,b,c], C. Changenet [b,*], F. Ville [a,*], M. Lalmi [c], S. Becquerelle [c]

[a] Université de Lyon, INSA de Lyon, LaMCoS, France
[b] Université de Lyon, ECAM Lyon, LabECAM, France
[c] SAFRAN Transmission Systems, Collombes, France

ARTICLE INFO

Article history:
Received 23 December 2016
Received in revised form 18 April 2017
Accepted 22 July 2017

Keywords:
Condition Monitoring
Fault detection
Temperature
Thermal behavior

ABSTRACT

Gear unit condition monitoring is a key factor for mechanical system reliability management. When they are subjected to failure, gears and bearings may generate excessive vibration, debris and heat. Vibratory, acoustic or debris analyses are proven approaches to perform condition monitoring. An alternative to those methods is to use temperature as a condition indicator to detect gearbox failure.

The review focuses on condition monitoring studies which use this thermal approach. According to the failure type and the measurement method, it exists a distinction whether it is contact (e.g. thermocouple) or non-contact temperature sensor (e.g. thermography). Capabilities and limitations of this approach are discussed. It is shown that the use of temperature for condition monitoring has a clear potential as an alternative to vibratory or acoustic health monitoring.

1. Introduction

Whether it is for high-speed gears, as in aeronautic transmissions, or low to medium speed, as in automotive applications, the trend in industry is to increase transmitted power and reduce weight of the mechanical systems. As a result, mechanical transmissions operate under more severe conditions.

Industrial fields such as transportation or energy production are very dependent on transmission reliability. Because of safety requirement or financial viability, breakdown times have to be more efficiently managed. Condition monitoring (CM) can be performed to improve mechanical systems availability and safety.

Accelerometers or any acoustic recording devices on the system are the most used methods to seek fault signatures. As a consequence, there is a tremendous amount of scientific studies that are conducted each year on this subject. Various signal treatment methods and numerical approaches are developed. The main difficulties of these approaches consist in: (i) extracting information from the highly noisy signal in gearboxes and (ii), identifying a fault signature.

In addition, different approaches also exists to perform gearbox CM: motor current spectrum analysis [1], transmission error [2] or oil analysis through particle counting and shape analysis [3,4] or measuring colorimetry or moisture pollution [5], etc. Because of complex instrumentation and data analysis, even if these methods are interesting, they remain difficult to use in an industrial context.

* Corresponding authors.
E-mail addresses: christophe.changenet@ecam.fr (C. Changenet), fabrice.ville@insa-lyon.fr (F. Ville).

http://dx.doi.org/10.1016/j.ymssp.2017.07.044
0888-3270/

Another possible approach consists in exploiting temperature measurement to detect abnormal gearbox operating conditions. This approach is based on the fact that all functioning mechanical systems generate power losses which induce temperature increase in the system. Therefore, assuming that a system presents degradation on contact surface, it will generate more power losses and then a different thermal behavior.

This paper is reviewing some studies on the use of temperature for condition monitoring and evaluates the capability of current methods to detect fault in gearboxes. The first part underlines the influence of defects on temperatures in gear units. The next sections review articles according to the measurement methodology and the application field. The last part synthetizes the reviewed studies and propose some conclusions.

2. Fault influence on temperatures

Typical gear units contain three main components: shafts, gears and bearings. Because of the interactions that take place at the contact of two moving parts, both gears and bearings generate power losses while operating. These losses can be separated into two main sources: the load dependent losses and the no-load dependent. Fig. 1 lists the dissipation sources generated by a gear or a rolling element bearing along with some literature example to estimate them.

No-load dependent losses are associated with the relative motion between a fluid and a solid surface. Lubricant trapping occurs when lubricant is pumped out of the gear meshing [6,7]. Air windage is due to the air being trapped and expelled of a rotating gear [8]. Oil churning takes place when rotating gears are partially immersed into lubricant and is due to oil circulation around them [9]. These losses depend on the macro-geometric parameters of the surface and may be impacted by system degradation that occurs at this scale: Such broken tooth, highly degraded rolling element of a bearing, etc. The load dependent losses take place at interaction between surfaces and lubricant where friction occurs. This is a micro-geometrical scale interaction that is mostly dependent on surface aspect, chemical interaction and operating conditions. In gear units, lots of the surface defects occur at this scale such micropitting, pitting, spalling or scuffing.

In a lubricated mechanism, contact interactions generate compression and shear stress into the material. These stresses will induce evolution in the component and its surface. Fig. 2 presents the global behavior of the surface during component life. Firstly, the surface quickly changes during a running in period. Then it reaches a second phase where it slowly evolves due to micro abrasion and wear. Finally the system may experience a mechanical failure that leads to sudden surface evolution.

Figs. 3 and 4 show two different surface defects that can occur on gear or rolling element bearing (REB). A surface defect can be localized, such as the spalling shown in Fig. 4 or distributed (e.g. micropitting on Fig. 3).

In addition to these surface failures other types of faults may occur in geared units. They can be classified into three different categories (named type 1, 2 or 3, hereafter) according to their origin:

1. Surface initiated damage. As presented previously and detailed in reviews performed by Olver [10] or Sadeghi [11], these defects can be localized, such as pitting, spalling or cracks, or distributed, such as scuffing and micropitting.
2. Geometrical induced problems, such as shaft unbalance or bearing misalignment.
3. Lubrication failure, such as lubrication starvation or lubricant contamination/pollution.

Under normal operating condition, gears are sources of power dissipation, one of these being tooth friction [12] which depends on surface features [12,13]. These ones are dependent on some type 1 defects such as micropitting [14,15]. As temperature is directly dependent on power losses, it may be impacted by surface failure.

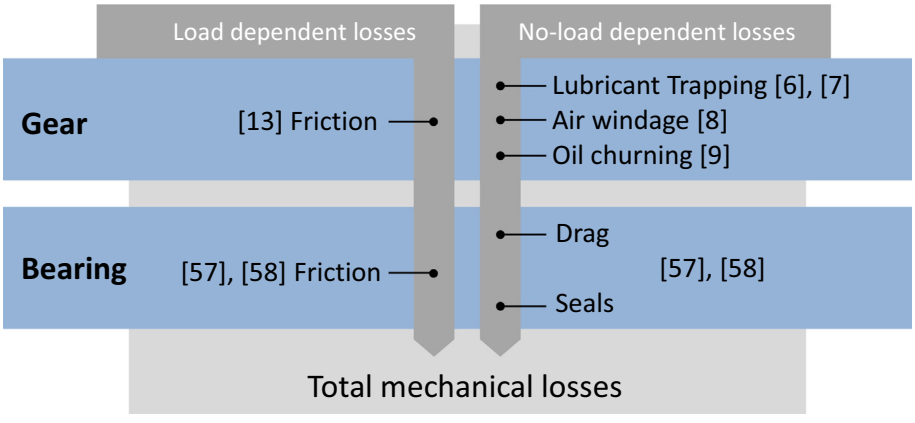

Fig. 1. Description of the losses partition in geared systems.

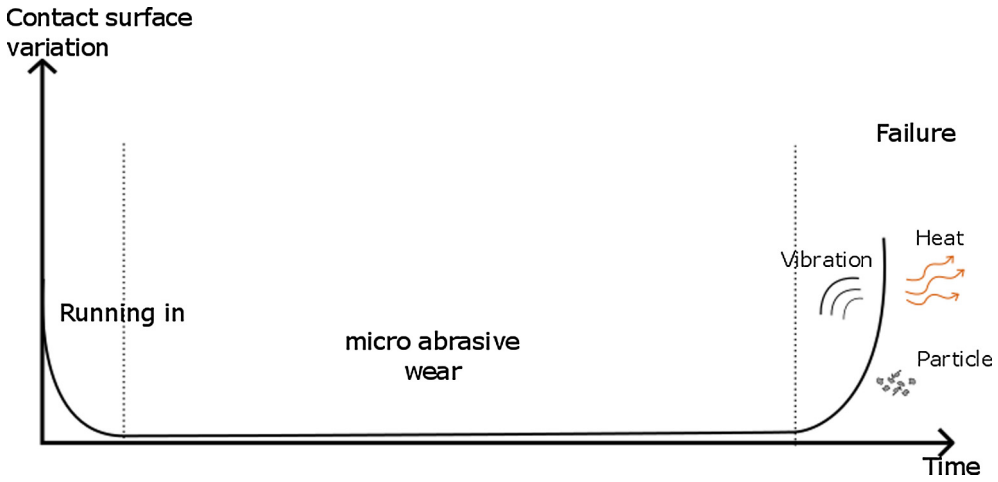

Fig. 2. contact surface variation from running into failure.

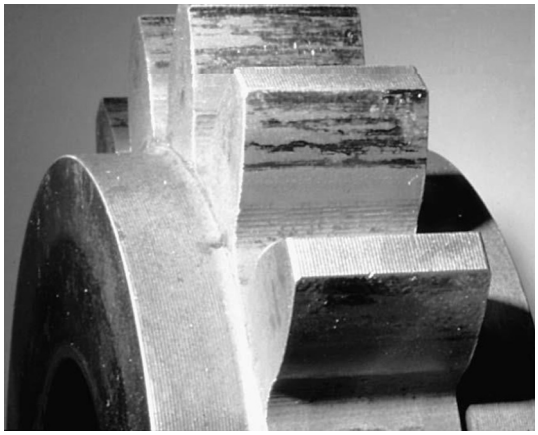

Fig. 3. Micropitting on a FZG gear [16].

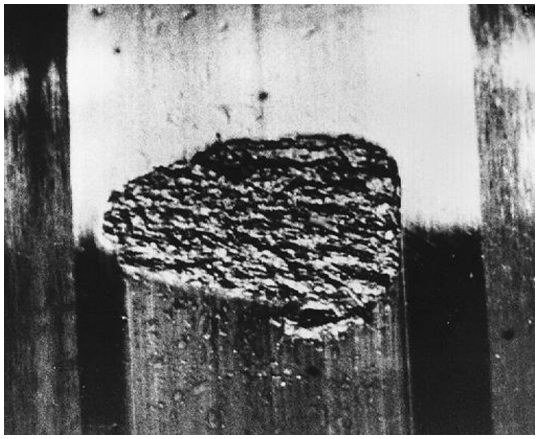

Fig. 4. Spalling on a bearing ring [57].

Type 2 fault category may increase the load supported by bearings and modify the contact area in gear mesh. This modifications lead to power losses increase without surface modification as for mechanical failures.

Finally lubricant play five different and complementary roles: transmit the loads, accommodate the contacting speeds, evacuate heat and reduce friction. When a type 3 failure occurs on a lubricated system, these functions are not effectively ensured and may both lead to temperature increase.

It can be also underlined that temperature has a noticeable effect on fault evolution. In fact, it can impact additive efficiency. This correlation was experimentally investigated by Hohn [16]. He concludes that temperature increase may lead to a reduction of failure evolution in gear if additives performance increases in the appropriate temperature range.

3. Type 1: Surface initiated damage

Both gears and bearings can be damaged and lead to a temperature increase. Nevertheless temperature measurements of these components are unequally difficult: gears are moving elements and so temperature measurements need specific strategies in order to retrieve it whereas measurements are easily possible on the bearing fixed parts such as outer rings.

3.1. Bearing condition monitoring

From previous studies, it appears that temperature measurement method influences diagnosis capabilities and method: data obtained from a thermography (temperature matrix) are different from the ones obtained from a contact sensor (single point measurement).

3.1.1. Contact sensor

Before trying to develop a full diagnosis methodology, the first approach consists in trying to detect temperature variation due to fault. To this end, a similar method is used in different studies: temperature measurement with failure or during its occurrence and seek for a difference with measurement from healthy system. To be comparable, experiments need to be performed for identical and controllable operating conditions. Laboratory studies fit these requirements as it is possible to control both the operating conditions and the test environment. Harvey [17] combined temperature and particle counting sensor to detect an artificially initiated fault on a 2500 rpm and 10 kN bearing test rig. 30 min prior to final failure a 5 °K increase is observable along with a significant particle count increase. Similar operating condition was used by Craig [18] with a 2700 rpm and 2.5 GPa Hertz pressure bearing test rig. A 5–10 °K increase is observed 9 h before spalling occurs (seeded with an indent on the raceway). Vibrational measurements and particle counting were also performed. It is shown that both of these methods had the same sensitivity to fault. Tarawneh et al. [19] tested railroad roller bearing in a speed range from 140 to 800 rpm and with a maximum applied load of 153 KN. Healthy bearing temperature was compared with inner and outer ring spalled bearing and averaged for each operating condition. It appeared that temperature rise was more significant with the inner ring defect (4 °K). Yet, this increase was close to the temperature disparity of a healthy bearing for a given operating condition. The link between defect size and temperature was investigated without being able to find a correlation. Howard [20] used a more powerful test rig reaching 1100 KN at 100 rpm to stick with wind turbine operating conditions. This bench allowed the development of natural fatigue spall on bearings. For the highest load a 3 °K increase is observable 1.5 h prior to the final failure. For all these studies, temperatures were measured on the bearing outer ring (Fixed one). Craig [18] and Howard [20] additionally measured the oil inlet and outlet temperatures.

For full size system, it is likely impossible to obtain repeatable conditions. So a predictive model is necessary to take into account operating conditions and estimate what should be temperatures under nominal conditions. Then it is necessary to analyze and to decide if a drift between measurements and simulations is due to a component failure. Various methods are available in the literature. Schlechtingen [21] developed a neural network model using 90 days of data from a healthy 2 MW wind turbine. The difference between simulation and measurement was averaged over a day to reduce the model uncertainty. The bearing is considered as damaged when the temperature difference overtakes the 1 °K threshold considered as fault representatives. The damage was detectable 70–180 days before failure. Kusiac [22] used similar approach with a 1.5 MW wind turbine. Compared to Schlechtingen the error between measurements and simulations was reduced using a moving average filter and a 2 °K threshold. Detectability was considerably reduced as fault was anticipated 1 h before occurring. The same kind of model was also employed by Bangalore [23]. The 2 MW wind turbine studied operated from 160 to 1500 rpm. This study used two different diagnostic approaches. The first one was based on a mean Mahalanobis distance calculation and is compared with a threshold. The other one was built on a component warning approach called Supervisory Control and Data Acquisition System (SCADA). The bearing presented a generalized surface damage on the outer ring when failure occurred (Fig. 5). This fault was clearly spotted by both the SCADA and Mahalanobis distance approach 45 days before breakdown as it can be seen on Fig. 6.

Garcia et al. [24] developed a much more complex data treatment method for a 700 kW studied wind turbine. The neural network employed to simulate the nominal gearbox behavior also estimated the confidence bands. These limits were used to define the defect representativeness and were around 5 °K. A diagnostic module based on fuzzy logic estimated if threshold overtaking was due to mechanical failure or not. The failure was detected 3 days before and leads to a 15 °K final temperature drift.

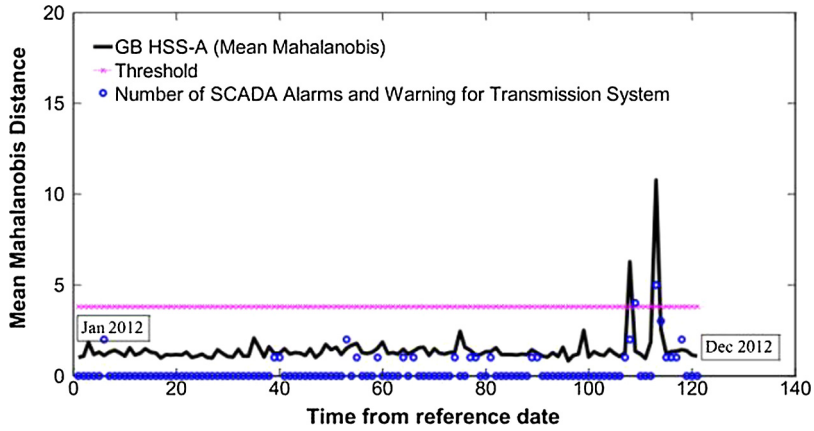

Fig. 5. One year average MD calculated with temperature [23].

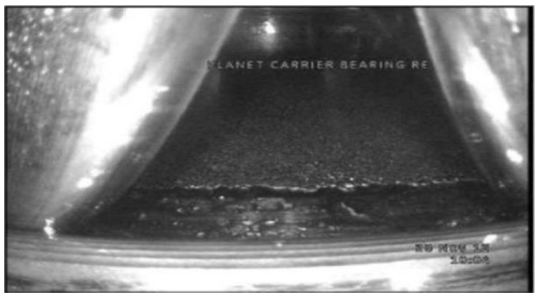

Fig. 6. Spalling on the Low speed bearing responsible of Gearbox failure [23].

Table 1
Synthesis for Bearing Health Monitoring with contact temperature sensors.

Reference	Measured part	Fault type	Test condition	Diagnostic method	Temperature variation	Fault detectability
Harvey 2007 [17]	Bearing	Type 1	2500 rpm 20 kN load	Experimental approach	Final: 5 °C	30 min
Craig 2010 [18]	Bearing Inlet oil Outlet oil	Type 1	2700 rpm 2.5 GPa max Hertz stress	Experimental approach	Trend: 5 °C Final: 10 °C	3 h
Tarawneh 2016 [19]	Bearing	Type 1	140–799 rpm 140 KN max load	Experimental approach	3–4 °C	Discussed
Howard 2015 [20]	Bearing	Type 1	100 rpm 1140 kN load	Experimental approach	3 °C	1.5 h
Schlechtingen 2011 [21]	Bearing Oil Ambient	Type 1, 2 and 3	1500 rpm (estimated) 2 MW	Threshold on average temperature	Trend: 5 °C	180 days
Kusiac 2012 [22]	Gearbox Oil Ambient	Probably type 1	1500 rpm 1.5 MW	Threshold on filtered temperature	Trend: 1.5 °C	1.5 h
Bangalore 2015 [23]	Bearing Oil Ambient	Type 1	From 160 to 1500 rpm 2 MW	Threshold on Mahalanobis mean and SCADA	Unknown	45 days
Garcia 2006 [24]	Bearing Oil Ambient	Probably type 1	1500 rpm (estimated) 700 kW	Temperature confidence bands and fuzzy inference	Trend: 5 °C Final: 15 °C	3 days

This temperature approach may also be a good solution for health monitoring of pad bearings. As these bearings use fluid as surface separator and polymer pads, it is impossible to perform some of the usual analyses such as electrostatic monitoring and vibrational monitoring is difficult because of oil film damping effect. Some studies investigated the effect of the pad surface feature on temperature [25] other performed monitoring using temperature measurements [26,27]. Only few results demonstrated a temperature increase due to actual excessive wear [28].

Table 1 summarizes reviewed articles, detailing operating conditions, diagnostic method, temperature increase and fault detectability.

3.1.2. Thermography

Thermography is another commonly used method for diagnostic using thermal measurement. It is based on the measurement of the infrared rays emitted by solids at a given temperature. The obtained spectrum is used to estimate the surface temperature of the considered elements. The main issue with this method is due to uncertainties introduced by lubrication, as oil may interfere with the infrared emission. Bagavathiappan et al. [29] described various industrial fields where thermography measurement was used for monitoring: electronic device, power plant, mechanical industry and housing. Despite not being descriptive about methodology, it gives a good overview of this approach for other fields than geared transmissions.

Compared to contact sensors that provide single point measurements, thermography allows estimating and visualizing the temperature distribution over the surface of a mechanical system. Experimental investigation [30] used the maximum temperature estimation. Grease lubricated bearing were running at speed from 1000 to 3000 rpm without load. A 20 °K difference could be observed between spalled and normal bearing. Kim [31] with similar setup and operating condition analyzed the temperature distribution between spalled and normal bearing. Fig. 9 shows the difference in temperature distribution according to fault type. This study also investigated the influence of excessive wear. It was quantified by measuring the raceway roughness. For the same operating condition a 7 °K increase was observable between lower and higher roughness. Mazioud [32] also performed experimental investigation on a bearing running at 1500 rpm. The impact of ring deformation on the temperature distribution and vibratory signal was measured. It has been shown that there is a link between temperature rise and vibration level according to the fault magnitude.

The previous study only investigates the fault detectability threw thermography measurements. Automatic analyses raise some issues concerning signal treatment due to the great amount of data generated by thermography. Younus [33] proposed a solution. Spalled and healthy bearing were tested on a 3450 rpm rig, no load was applied. Each temperature measurements point (thermograph pixel) was classified using a histogram. Then form factors such mean, standard deviation and skewness were estimated from this temperature histogram. Additional data treatment algorithm was used as these parameters were not sensitive enough: the Independent Component Analysis (ICA) and Principal Components Analysis (PCA). It estimates parameter correlation representativeness in data set. Finally considering the ICA and PCA parameters a good discrimination was obtained between faulted and normal bearing. Tran [34] used the same test bench and operating conditions but performed the data treatment (empirical mode decomposition) before the form factor estimation. Fuzzy logic was used in addition to analyze the form factors and automatically provide a diagnostic. Janssens [35] used the same approach to detect bearing fault on a test rig that runs at 1500 rpm. He studied outer ring fault consisting of "shallow grooves" represented on Fig. 7. As with Tran, the image is pretreated before computing the form factors. The diagnosis was performed into three steps: (i) the variation of the thermal image was computed; (ii) one-dimension temperature variation histograms were calculated from this image; and (iii) the form factors were extracted from these histograms. Finally the diagnosis was done by manually analyzing these factors. The same discrimination capability as Tran and Younous was obtained. Janssens [36] recently proposed an extension to his previous work. Fault combinations are detected with a novel automated method. With this extended approach, a lower detectability of a bearing outer race fault is observed (55% accuracy) compared with Type 2

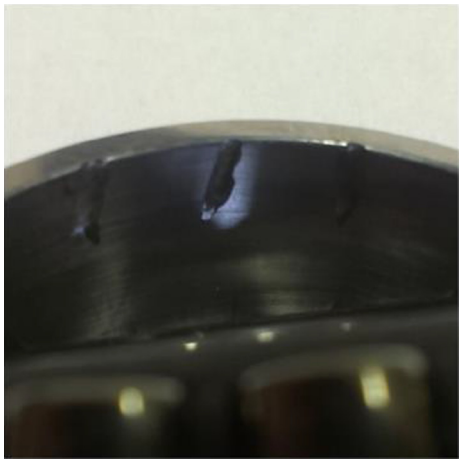

Fig. 7. Outer ring shallow grooves from Janssens [35] Study.

Table 2
Synthesis for bearing thermography analysis.

Reference	Measured part	Fault type	Test condition	Diagnostic method	Temperature variation
Dongyeon 2010 [30]	Bearing Shaft	Type 1 and 2	1000–3000 rpm No load	Location of temperature increase	Spalling: 10 °C Lub loss: 15 °C
Kim 2012 [31]	Bearing Shaft	Type 1 and 2	1000–3000 rpm 10–50 N	Location of temperature increase	Spalling: 20 °C Wear: 5–20 °C
Mazioud 2008 [32]	Bearing	Type 1	1500 rpm No load	Max temperature	NA
Younus 2010 [33]	Bearing Shaft	Type 1 and 3	3750 rpm No load	Thermography form factor analysis + data treatment	NA
Tran 2013 [34]	Bearing Shaft	Type 1 and 3	3750 rpm No load	Thermography form factor analysis + fuzzy logic	NA
Janssens 2015 [35]	Bearing	Type 1, 2 and 3	1500 rpm No load	Manual Thermography form factor analysis	NA
Janssens 2017 [36]	Bearing	Type 1, 2 and 3	1500 rpm No load	Automated thermography form factor analysis	NA
Widodo 2016 [37]	Bearing Shaft	Type 1 and 3	1800 rpm No load	Thermography form factor analysis	NA
Leemans 2011 [38]	Casing Bearing Ambient	Type 1	2600, 5500 and 9000 rpm 500 KW	Temperature threshold	Trend: 1.5 °C
Bagavathiappan 2013 [39]	Bearing Shaft Belt	Type 1	980 rpm 75 kW	Hot spot detection	Trend: 8 °C

or 3 faults (82.5% accuracy). Widodo et al. [37] tested bearings at 1800 rpm without load. The thermal image was computed to determine the temperature variation threshold. Those thresholds drew area and perimeters corresponding to isotemperatures. They were used as decision variables for diagnosis in addition with other classical form factors. All the diagnostic variables were analyzed using a neural network. It was trained with healthy and faulted bearing to detect the fault signatures in the decision parameters.

As with single point measurements, investigating full size systems present new problematics due to the least controllability of the ambient parameters and operating conditions. A model is used to overcome the problem. Leemans [38] study focused on an industrial blower. This device was associated with a 500 kW electric motor operating at 2600, 5500 and 9000 rpm. Detection of bearing excessive wear was investigated. The mean temperatures of several thermograph zones were compared. Each one was considered as representative of component health. Ambient temperature and generated power were chosen as input variables not to be influenced by the day/night and summer/winter cycles. Considering this model and using a 1.5 °C threshold, the temperature drift due to bearing wear seems detectable. Authors did not investigate the prediction capability given by this method. Bagavathiappan et al. [39] also performs health monitoring on industrial blowing system. In this application, the system was operated by a 75 kW motor at 980 rpm. The diagnostic approach was tested with a spalled bearing. This work investigated the temperature distribution on the bearing casing, and more specifically, the values of the hottest spots. Finally, the spalled bearing implied a temperature increase equal to 8 K.

Table 2 summarizes reviewed studies, stating operating conditions, diagnostic methods and temperature increase.

3.2. Gear condition monitoring

Gear diagnostic is much more difficult than bearing one due to the complexity to measure gear temperature: it is difficult to place a sensor at the tooth contact of a rotating gear or use thermography due to lubricant. A solution is to use indirect health indicators.

3.2.1. Contact sensor

Using contact sensors, the classical indirect approach consists in measuring oil temperature which depends on power losses and may increase with gear damage. As measurement is indirect a model is necessary to estimate if temperature drift is caused by failure or environment modifications. Feng [40] developed a model based on power losses to estimate the global lubricant temperature rise. A 2 Mw wind turbine gearbox was equipped with thermocouples on oil circuit and high speed shaft bearings along with vibration sensors and particle counter. 3 months before failure and almost 1 month before the threshold overcome of other types of sensor, a 5 °K temperature rise was observed. The author concludes on the equal capability between temperature and vibration measurement to detect fault occurring in wind turbine gearboxes. Qiu [41] used the same approach on a 1.5 MW wind turbine gearbox operating at 1500 rpm. A thermomechanical model was developed. Unlike Feng, the diagnostic was made by computing the efficiency from temperature measurement. With this approach a clear decrease in efficiency, and therefore, a 3-5 °K temperature increase, was observed 3 month prior to failure. Wang [42] and Zhao [43] both used autoregressive model fitted with measurements from healthy wind turbine. For Wang [42],

the fault criterion was based on model residual error standard deviation (SD) and alarm threshold was chosen as three times the SD. Zhao [43] exploited the differences between measured and simulated temperatures of oil, high speed shaft bearing and main shaft bearing. They were compiled into a single detecting function. He considered that the gearbox was damaged when the function value overcome a certain threshold. In this study, it corresponded to a 4 °K gearbox temperature increase. Infield and Wang [44] trained a "non-Parametric non-linear model" to estimate gearbox oil temperature. Residual between model and measurement was filtered through a low pass filter. A 1 °K deviation was considered as fault representative and raised alarms. With one of the studied case first alarm was raised 10 days before shutdown and allowed to detect upcoming gearbox failure. Finally, Zaher et al. [45] studied wind turbine gearboxes that operated from 150 to 1500 rpm at 600 kW. A neural network was used to estimate the oil and bearing temperatures as a function of the generated power and nacelle temperature. 3 months of data were used to train the neural network. A clear increase of the oil temperature was observed 6 months prior to failure, along with a very low increase of bearing temperature. Measurement and simulation were both compared and analyzed by a Multi Agent System. Temperature measurements from different parts of the gearbox with ambient condition were evaluated to estimate the root cause of temperature rise based on expert rules. It analyzed abnormalities and automatically informed the operator on the wind turbine condition.

3.2.2. Thermography

Diagnostic difficulty is mainly caused by the use of oil as it interferes with surface emissivity measured with camera. An experimental investigation performed by Waqar et al. [46] used thermography to detect faults on a worm gear by measuring casing temperature. The wheel presents a chipped tooth. Two speeds are tested (1440 and 1920 rpm) with two different oil level. Diagnosis was performed by a neural network. It was trained by testing ten times all operating conditions with nominal and damaged gear. At 1920 rpm and with a 50 ml oil volume, the gearbox housing temperature is increased by 5 °K. This study shows that it is possible to detect gear failure through indirect measurement of the casing temperature with dip lubrication. Table 3 compiles all the data about gear condition monitoring.

4. Type 2 and 3: geometrical defect and lubrication failure

Most of the geometrical failure (type 2) implies load increase on components that may leads to loss increase. For the lubrication failure (type 3) temperature increase is caused by the combination of power losses increase and diminution of cooling efficiency.

4.1. Geometrical defect

Different types of geometrical defect such shaft misalignment or unbalance and incorrectly mounted bearing were reviewed. The study performed by Tonks et al. [47] investigated the detection of shaft misalignment. The experimentation was performed at 50 rpm without load. The set up allowed the authors to adjust the position of two bearings to modify the misalignment. For low speed and no torque, a temperature difference was observed between nominal condition and misaligned shaft. For severe misalignment, temperature raised up to 2 or 3 K. The authors concluded on the capability of temperature measurement to detect shaft misalignment but also highlighted the influence of ambient temperature. Mohanty [48] used the same kind of setup to study shaft misalignment by moving bearing casing. Thermocouples were placed on the bearing outer rings. Higher speed than Tonks were tested (1740 and 2220 rpm) and load was applied by adding a 5 kg mass on the shaft. Finally, a 1 °K increase was noticed on stabilized temperature. An increase on the temperature gradient was also

Table 3
General synthesis for Gear Diagnostic.

Reference	Measured part	Fault type	Test condition	Diagnostic method	Temperature variation	Fault detectability
Feng 2013 [40]	Bearing Oil	Probably type 1	From 160 to 3000 rpm 2 MW	Threshold on average temperature	Trend: 5 °C	90 days
Qiu 2016 [41]	Oil	Type 1	1500 rpm 1.5 MW	Expert system rules on efficiency	Trend: 5–10 °C	90 days
Wang 2012 [42]	Oil	Probably type 1	NA	Threshold on model error standard deviation	NA	NA
Zhao 2012 [43]	Oil High speed and main shafts bearings	Probably type 1	NA	Model/simulation Error function	4 °C	NA
Wang 2013 [44]	Oil	Probably type 1	NA	Threshold on filtered temperatures	1 °C	10 days
Zaher 2009 [45]	Oil Bearing	Probably type 1	1500 rpm 600 kW	Expert system	Trend: 3–5 °C	6 month
Waqar 2016 [46]	Casing	Type 1	1440 and 1920 rpm No load	Neural network	Trend: 5 °C	NA

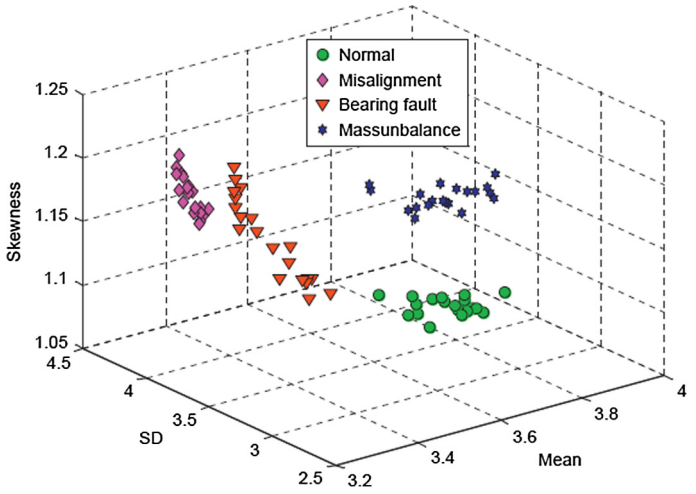

Fig. 8. Tran's [34] form factor with image treatment.

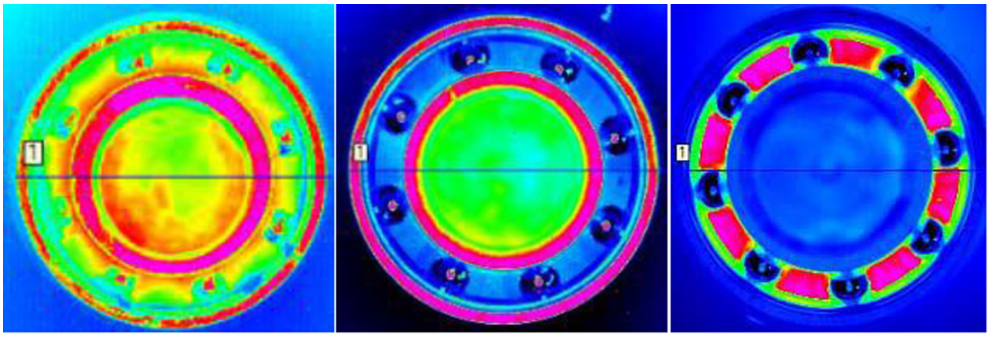

Fig. 9. Normal, starved and spalled bearing at 1000 rpm.

observed in the presence of defect. No specific correlation was found between the temperature increase due to defect and the speed or the applied load. Jedrzejrwski [49] explored the detectability of bearing incorrect sealing of a machining tool spindle. The shaft was running at different speeds from 500 up to 1500 rpm, but no information was given about the bearing load. This study was based on a model to estimate the nominal temperature and to provide minimum/maximum temperature thresholds. With incorrectly sealed bearing a temperatures rise from 3 to 10 K above the computed maximum limit depending on the rotational speed was noticed.

Thermography also permits to investigate geometrical defects. Studies by Younus [33], Tran [34] and Janssens [35,36] presented in the type 1 section also investigated bearing misalignment and shaft unbalance. It appears that the form factor approach they used not only allowed to differentiated normal from faulted system but also differentiate the defect type. As in the type 1 section Younous [33] needed to perform the PCA and ICA computation to obtain clear separation between fault types. The signal treatment employed to differentiate normal from faulted behavior by Tran [34] and Janssens [35] also discriminates fault types from one to another. Fig. 8 shows the clustering of the form factors computed by Tran [34] according to the fault. Similar representations were obtained by Younus and Janssens. Table 4 summarizes the Type 2 fault results.

Ramirez [50] used a 2.5 KW test rig running at 3600 rpm coupling motor, gearbox and generator. Fault was added by unbalancing the motor shaft. Infrared camera raw data were processed with inner and outer temperature sensors from the test bench. The obtained thermographs were analyzed to estimate the bearing and gearboxes characteristic temperatures. As a result, the temperature rise between healthy and faulted bearing reach 1.5 °K with optimum data processing (outer temperature as reference).

Table 4 summarizes the reviewed Type 2 faults results.

4.2. Lubrication failure

Very few studies deal with lubrication failure all are conducted by thermography analysis. Lopez-Perez [51] presented case studies of three different generator bearings showing abnormal temperature due lubrication failure. The threshold temperature was fixed at 70 °C. Faulted bearing temperatures were measured between 100, 90 and 80 °C depending on the lubri-

Table 4
Summary of the study on the Type 3 fault.

Reference	Fault type	Test condition	Diagnostic method	Temperature variation
Tonks 2016 [47]	Type 2	50 rpm No load	Experimental approach	Trend: 1–3 °C
Mohanty 2015 [48]	Type 2	1740 and 2220 rpm 5 kg mass	Experimental approach	Trend: 1 °C
Jedrezejrwski 1985 [49]	Type 2	1500 rpm	Computed temperature limit	Trend: 5–15 °C
Younus 2010 [33]	Type 1 and 2	3750 rpm No load	Thermograph form factor analysis + data treatment	NA
Tran 2013 [34]	Type 1 and 2	3750 rpm No load	Thermograph form factor analysis + fuzzy logic	NA
Janssens 2015 [35]	Type 1,2 and 3	1500 rpm No load	Thermograph form factor analysis	NA
Ramirez 2016 [50]	Type 2	3600 rpm 2.5 kW	Thermograph region analysis	1.5 °C

Fig. 10. Low and adequate lubrication from Janssens [35] study.

cation loss severity. Kim [31] and Dongyeon [30] used their bearing test bench under starved conditions. Temperature distribution was different according to the failure type in Kim's experiments (Fig. 9). The outer ring is hotter under starved conditions compared with nominal ones whereas the cage temperature is the hotter part for the spalled bearing.

Dongyeon made the same global observation and also measured and compared the maximum temperatures. Under starved conditions, a 10–15 °K increase was observed on the outer ring. Janssens [35] investigated the effect of grease quantities on lubrication and the temperature distribution in bearings (Fig. 10). As in the previous studies form factor estimated from the thermograph histogram revealed differences between a healthy bearing and an incorrectly lubricated one. Table 5 collects all the information from studies about type 3 defect.

5. Discussion

In the previous sections, several studies exploiting temperature measurements to perform condition monitoring have been presented. As literature is limited compared to vibrational or acoustic approaches, an emphasis has been given to technical specificities. The objective was to seek for general capabilities and limitations of the temperature monitoring approach. Some remarks can be drawn from this review:

- It is possible to diagnose gear defect through indirect temperature measurement [22,40,41,45]. To this end, the oil or casing temperature can be used.
- The use of temperature average or filtering methods seems to improve fault detectability [19,21,23,40,41,44,45]. The methods employed are defined in Table 6.
- Form factor is widely used with thermography because it makes possible to analyze a high number of measurement points with few parameters. This method is able to discriminate between wide varieties of faults [33–35,37].
- None of these studies performed thermography along time to develop an online method to detect or anticipate fault. The amount of data which are included in a single thermography image can explain this observation. Indeed, the recording of different images for a long time-period would generate a huge amount of data. This problem may be overcome by recording form factors rather than raw images.

Table 5
Studies exploring the Type 3 defect.

Reference	Fault type	Test condition	Diagnostic method	Temperature variation	Fault detectability
Lopez-Perez 2016 [51]	Type 3	NA	Location of temperature increase	10–30 °C	NA
Dongyeon 2010 [30]	Type 1 and 3	1000–3000 rpm No load	Location of temperature increase	Spalling: 10 °C Lub loss: 15 °C	NA
Kim 2012 [31]	Type 1 and 3	1000–3000 rpm 10–50 N	Location of temperature increase	Spalling: 20 °C Wear: 5–20 °C	NA
Janssens 2015 [35]	Type 1,2 and 3	1500 rpm No load	Thermography form factor analysis	NA	NA

Table 6
Summary of the experimental data processing methods employed.

Reference	Experimental data processing method employed
Tarawneh [19]	Operating condition average
Schlechtingen [21]	One day measurement average
Bangalore [23]	Mean Mahalanobis distance
Feng [40]	Operating condition average
Qiu [41]	10 min average
Wang [44]	Infinite impulse response low pass filter
Zaher [45]	1 h or 10 min average

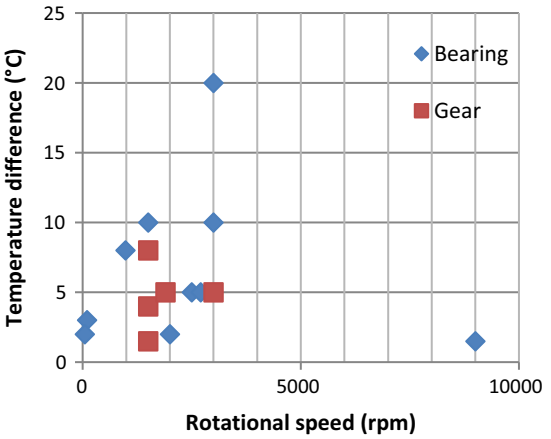

Fig. 11. Plot of the temperature increase due to fault versus rotational speed of the mechanical element.

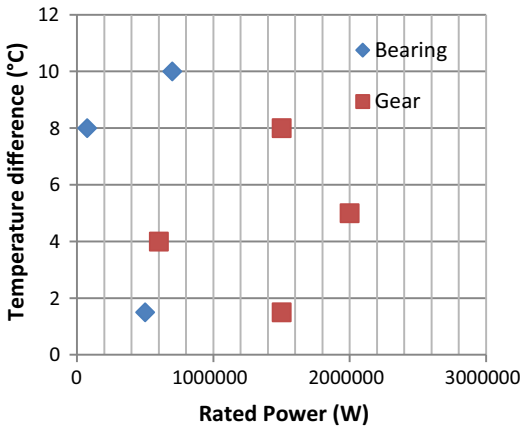

Fig. 12. Plot of the temperature increase due to fault versus rated power of the system.

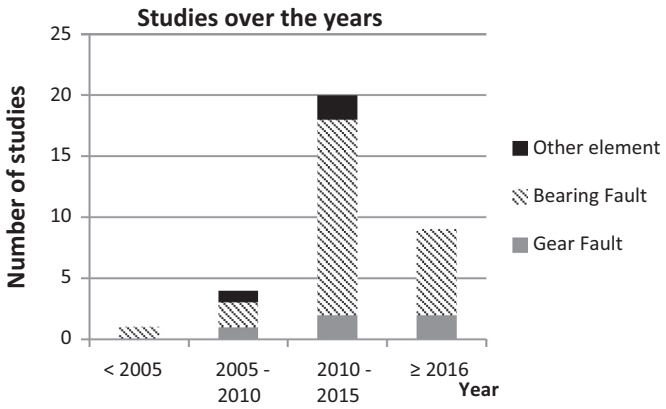

Fig. 13. Studies repartition over time.

Table 7
Types of faults studied in the reviewed articles.

		Type 1: (surface defect)	Type 2: (Lubrication failure)	Type 3: (Geometrical issues)
Punctual measurement	Experimental	[17,20,18,42–44,53,28]		[47,48]
	Industrial	[40,41,45,22,21,24,23,19]	[21]	[49,21]
Thermography measurement	Experimental	[30–32,54–56,33–36,46,37]	[30,31,34,35,50]	[33–35,37,51]
	Industrial	[38,39]		

- Fig. 11 shows that no clear correlation has been found between the rotational speed and final temperature increase of a faulted gear unit (the fault may be located on gear or bearing).
- The rated power is neither a significant parameter for temperature increase as shown in Fig. 12. However, it seems that more transmitted power is required to perform temperature health monitoring on a gear rather than a bearing.
- In most of the studies, operating speed is under 3000 rpm and high load applications are considered. A single paper [52] used temperature monitoring for high speed gearbox. It was not detailed in this review because no relevant information was provided about employed system or method.
- Two similar geared units were used at different operating speeds. As a result, the relative temperature increase due to shaft misalignment was not dependent on the operating speed [18,19]. It seems that temperature rise due to fault is not correlated to shaft speed in the case of misalignment.
- Fig. 13 shows that there is an increased interest for temperature condition monitoring over the years.
- In the introduction section, different fault categories were listed according to the consequences for the thermal behavior. Table 7 presents the repartition of the investigated fault type in the studies. In the past years, surface defects have drawn most of the attention.

6. Conclusions

The reviewed literature shows that temperature health monitoring has a clear potential as an alternative to vibrational or acoustic health monitoring. By measuring temperature in a gearbox it is possible to detect various defects that may occurs such as bearing spalling, bearing excessive wear, gear defect, bearing misalignment, unbalanced shaft or lubrication losses.

Thermocouple measurement has some advantages: the cost is limited compared to vibrational analysis and easy to implement in line. By measuring oil temperature it is possible to assess the state of some elements without directly measuring them. But reliable information may only be obtained using a model to compare measurements with. It avoids the negative influence of operating changes or exteriors event that may lead to false diagnostic.

Thermography may be preferable for systems were a lot of empty space is available around the system as it allows identifying different faults with a single measurement. But with this method a complex data treatment method has to be implemented as two thermographs are difficult to compare from one to another. Future works are necessary to investigate the capability of this approach for others field such aeronautics or ground transportation.

Nowadays best detection capability is obtained using punctual measurement with data driven model and expert system diagnostic tool on wind turbines gearboxes. With this approach temperature measurement can spot occurring fault several month before catastrophic failure.

References

[1] N. Feki, G. Clerc, P. Velex, Gear and motor fault modeling and detection based on motor current analysis, Electr. Power Syst. Res. 95 (2013) 28–37.
[2] N. Feki, J. Cavoret, F. Ville, P. Velex, Gear tooth pitting modelling and detection based on transmission error measurements, Eur. J. Comput. Mech./Revue Eur. Mécanique Numérique 22 (2–4) (2013) 106–119.
[3] S. Ebersbach, Z. Peng, N.J. Kessissoglou, The investigation of the condition and faults of a spur gearbox using vibration and wear debris analysis techniques, Wear 260 (1–2) (2006) 16–24.
[4] Z. Peng, N. Kessissoglou, An integrated approach to fault diagnosis of machinery using wear debris and vibration analysis, Wear 255 (7–12) (2003) 1221–1232.
[5] I. Akira, New condition monitoring method of oil and machine elements by lubricant color analysis, in: STLE Annual Meeting, 2016.
[6] Y. Diab, F. Ville, P. Velex, Investigations on power losses in high-speed gears, Proc. Inst. Mech. Eng. Part J J. Eng. Tribol. 220 (3) (2006) 191–198.
[7] S. Seetharaman, A. Kahraman, Load-independent spin power losses of a spur gear pair: model formulation, J. Tribol. 131 (2) (2009) 22201.
[8] S. Pallas, Y. Marchesse, C. Changenet, F. Ville, P. Velex, A windage power loss model based on CFD study about the volumetric flow rate expelled by spur gears, Mech. Ind. 13 (2012) 317–323.
[9] C. Changenet, G. Leprince, F. Ville, P. Velex, A note on flow regimes and churning loss modeling, J. Mech. Des. 133 (12) (2011) 121009.
[10] A.V. Olver, The mechanism of rolling contact fatigue: an update, Proc. Inst. Mech. Eng. Part J J. Eng. Tribol. 219 (5) (2005) 313–330.
[11] F. Sadeghi, B. Jalalahmadi, T.S. Slack, N. Raje, N.K. Arakere, A Review of Rolling Contact Fatigue, J. Tribol. 131 (4) (2009) 41403.
[12] ISO, Gears - Thermal Capacity Part 2: Thermal Load-Carrying Capacity, 2001.
[13] Y. Diab, F. Ville, P. Velex, Prediction of power losses due to tooth friction in gears, Tribol. Trans. 49 (2) (2006) 260–270.
[14] R. Martins, C. Locatelli, J. Seabra, Evolution of tooth flank roughness during gear micropitting tests, Ind. Lubr. Tribol. 63 (1) (2011) 34–45.
[15] M. Amarnath, S.-K. Lee, Assessment of surface contact fatigue failure in a spur geared system based on the tribological and vibration parameter analysis, Measurement 76 (2015) 32–44.
[16] B.R. Höhn, K. Michaelis, Influence of oil temperature on gear failures, Tribol. Int. 37 (2) (2004) 103–109.
[17] T.J. Harvey, R.J.K. Wood, H.E.G. Powrie, Electrostatic wear monitoring of rolling element bearings, Wear 263 (7–12) (2007) 1492–1501, SPEC. ISS..
[18] M. Craig, Advanced Condition Monitoring to Predict Rolling Element Bearing Wear Using Multiple In-line and Off-line Sensing, Southampton, 2010.
[19] C.M. Tarawneh, L. Sotelo, A.A. Villarreal, N. de los Santos, R.L. Lechtenberg, R. Jones, Temperature profiles of railroad tapered roller bearings with defective inner and outer rings, in: 2016 Joint Rail Conference, 2016, p. V001T06A018.
[20] T.P. Howard, Development of a Novel Bearing Concept for Improved Wind Turbine Gearbox Reliability, University of Sheffield, 2015.
[21] M. Schlechtingen, I. Ferreira Santos, Comparative analysis of neural network and regression based condition monitoring approaches for wind turbine fault detection, Mech. Syst. Sig. Process. 25 (5) (2011) 1849–1875.
[22] A. Kusiak, A. Verma, Analyzing bearing faults in wind turbines: a data-mining approach, Renew. Energy 48 (2012) 110–116.
[23] P. Bangalore, L.B. Tjernberg, An artificial neural network approach for early fault detection of gearbox bearings, IEEE Trans. Smart Grid 6 (2) (2015) 980–987.
[24] M.C. Garcia, M.A. Sanz-Bobi, J. del Pico, SIMAP: intelligent system for predictive maintenance. Application to the health condition monitoring of a windturbine gearbox, Comput. Ind. 57 (6) (2006) 552–568.
[25] S.B. Glavatskih, M. Fillon, R. Larsson, The significance of oil thermal properties on the performance of a tilting-pad thrust bearing, J. Tribol. 124 (2) (2002) 377.
[26] S.B. Glavatskih, Ö. Uusitalo, D.J. Spohn, Simultaneous monitoring of oil film thickness and temperature in fluid film bearings, Tribol. Int. 34 (12) (2001) 853–857.
[27] S.B. Glavatskih, A method of temperature monitoring in fluid film bearings, Tribol. Int. 37 (2) (2004) 143–148.
[28] J. Zhou, Temperature monitoring of PEEK bearings, in: 71st STLE Annual Meeting and Exhibition, 2016.
[29] S. Bagavathiappan, B.B. Lahiri, T. Saravanan, J. Philip, T. Jayakumar, Infrared thermography for condition monitoring - a review, Infrared Phys. Technol. 60 (2013) 35–55.
[30] K. Dongyeon, Fault diagnosis of ball bearings within rotational machines using the infrared thermography method, J. Kor. Soc. Nondestruct. Test. 30 (2010).
[31] W. Kim, J. Seo, D. Hong, Infrared thermographic inspection of ball bearing; condition monitoring for defects under dynamic loading stages, in: Word Conference on Nondestructive Testing (2012) 4–7.
[32] A. Mazioud, L. Ibos, A. Khlaifi, J.F. Durastanti, Detection of rolling bearing degradation using infrared thermography, in: Proceedings of the 2008 International Conference on Quantitative InfraRed Thermography, vol. 1, 2008.
[33] A.M. Younus, A. Widodo, B.-S. Yang, Evaluation of thermography image data for machine fault diagnosis, Nondestruct. Test. Eval. 25 (3) (2010) 231–247.
[34] V.T. Tran, B.S. Yang, F. Gu, A. Ball, Thermal image enhancement using bi-dimensional empirical mode decomposition in combination with relevance vector machine for rotating machinery fault diagnosis, Mech. Syst. Sig. Process. 38 (2) (2013) 601–614.
[35] O. Janssens, R. Schulz, V. Slavkovikj, K. Stockman, M. Loccufier, R. Van de Walle, S. Van Hoecke, Thermal image based fault diagnosis for rotating machinery, Infrared Phys. Appl. 73 (2015) (2015) 78–87.
[36] O. Janssens, M. Loccufier, R. Van de Walle, S. Van Hoecke, Data-driven imbalance and hard particle detection in rotating machinery using infrared thermal imaging, Infrared Phys. Technol. 82 (2017) 28–39.
[37] A. Widodo, D. Satrijo, T. Prahasto, G.M. Lim, B.K. Choi, Confirmation of thermal images and vibration signals for intelligent machine fault diagnostics, Int. J. Rotat. Mach. 2012 (2012).
[38] V. Leemans, Evaluation of the performance of infrared thermography for on-line condition monitoring of rotating machines, Engineering 3 (10) (2011) 1030–1039.
[39] S. Bagavathiappan, T. Saravanan, N.P. George, J. Philip, T. Jayakumar, B. Raj, Condition monitoring of exhaust system blowers using infrared thermography, Insight Non-Destruct. Test. Cond. Monit. 50 (9) (2008) 512–515.
[40] Y. Feng, Y. Qiu, C.J. Crabtree, H. Long, P.J. Tavner, Monitoring wind turbine gearboxes, Wind Energy 16 (5) (Jul. 2013) 728–740.
[41] Y. Qiu, Y. Feng, J. Sun, W. Zhang, D. Infield, Applying thermophysics for wind turbine drivetrain fault diagnosis using SCADA data, IET Renew. Power Gen (2016) 1–8.
[42] F.F. Wang, X.Q. Xiao, H.S. Zhao, Wind turbine gearbox failure prediction based on time series analysis and statistical process control, Adv. Mater. Res. 347–353 (2011) 2236–2240.
[43] Hong-Shan Zhao, Xiao-Tian Zhang, Early fault prediction of wind turbine gearbox based on temperature measurement, in: 2012 IEEE International Conference on Power System Technology (2012) 1–5.
[44] D. Infield, Y. Wang, Supervisory control and data acquisition data-based non-linear state estimation technique for wind turbine gearbox condition monitoring, IET Renew. Power Gen. 7 (4) (2013) 350–358.
[45] A. Zaher, S.D.J. McArthur, D.G. Infield, Y. Patel, Online wind turbine fault detection through automated SCADA data analysis, Wind Energy 12 (6) (Sep. 2009) 574–593.
[46] T. Waqar, M. Demetgul, Thermal analysis MLP neural network based fault diagnosis on worm gears, Measurement 86 (2016) 56–66.
[47] O. Tonks, Q. Wang, The detection of wind turbine shaft misalignment using temperature monitoring, CIRP J. Manuf. Sci. Technol. (2016) 1–9.
[48] A.R. Mohanty, S. Fatima, Shaft misalignment detection by thermal imaging of support bearings, IFAC Proc. 48 (21) (2015) 554–559.
[49] J. Jedrzejewski, W. Kwasny, D. Milejski, M. Szafarczyk, Selected diagnostic methods for machine tools acceptance tests, CIRP Ann. - Manuf. Technol. 34 (1) (1985) 343–346.

[50] J.A. Ramirez-Nunez, S. Member, L.A. Morales-hernandez, R.A. Osornio-Rios, J.A. Antonino-Daviu, S. Member, R.J. Romero-Troncoso, S. Member, Self-Adjustment Methodology of a Thermal Camera for Detecting Faults in Industrial Machinery, 2016, pp. 7119–7124.
[51] D. Lopez-Perez, J. Antonino-Daviu, Detection of mechanical faults in induction machines with infrared thermography: field cases, in: IECON 2016 - 42nd Annual Conference of the IEEE Industrial Electronics Society, 2016, pp. 7107–7112.
[52] L. Xu, C. Zhang, H. Wang, X. Li, Y. Shen, Z. He, A.C. Analysis, A Method of Health Monitoring on Helicopter Speed Reducer Based on FMECA, 2016.
[53] L. Burstein, L. Segal, Prediction of machine residual service life: Method and computing, NDT E Int. 37 (7) (2004) 517–523.
[54] N. Ranc, D. Wagner, P.C. Paris, Study of thermal effects associated with crack propagation during very high cycle fatigue tests, Acta Mater. 56 (15) (2008) 4012–4021.
[55] Y. Gao, G.Y. Tian, K. Li, J. Ji, P. Wang, H. Wang, Multiple cracks detection and visualization using magnetic flux leakage and eddy current pulsed thermography, Sens. Actuat., A Phys. 234 (2015) 269–281.
[56] G. Degallaix, P. Dufrenoy, J. Wong, P. Wicker, F. Bumbieler, Failure mechanisms of TGV brake discs, in: Key Eng. Mater., vol. 345–346 I, 2007, pp. 697–700.
[57] AFNOR, ISO 15243: 2004-08, Roulements: Détérioration et défaillance, 2015.